

# Ecological and evolutionary implications of starvation and body size

1 **Justin D. Yeakel \* †‡, Christopher P. Kempes †, and Sidney Redner †§**

4 \*School of Natural Science, University of California Merced, Merced, CA, †The Santa Fe Institute, Santa Fe, NM, §Department of Physics, Boston University, Boston

5 MA, and ‡ To whom correspondence should be addressed: jdyeakel@gmail.com

6 Submitted to Proceedings of the National Academy of Sciences of the United States of America

## 7 This is the abstract.

8 The behavioral ecology of most, if not all, organisms is in-  
9 fluenced by the energetic state of individuals, which directly  
10 influences how organisms invest reserves in uncertain environ-  
11 ments. Such behaviors are generally manifested as trade-offs  
12 between investing in somatic maintenance and growth or al-  
13 locating energy towards reproduction [1, 2, 3]. The timing of  
14 these behaviors is often important and is under strong selective  
15 pressure, as it tends to directly impact future fitness [4]. Im-  
16 portantly, the influence of resource limitation on an organism's  
17 ability to maintain its nutritional stores may lead to repeated  
18 delays or shifts in reproduction over the course of an organism's  
19 life.

20 Maximizing fitness between growth and maintenance activi-  
21 ties vs. reproduction structures the life-history of many species,  
22 and this can be achieved by alternative behavioral strategies  
23 conditioned on resource availability [5]. For example, reindeer  
24 invest less in calves born after harsh winters (when the mother's  
25 energetic state is poor) than in calves born after moderate win-  
26 ters [6], whereas many bird species invest differently in broods  
27 during periods of resource scarcity [7, 8], sometimes delaying  
28 or foregoing reproduction for a breeding season [1, 9, 10]. Even  
29 freshwater and marine zooplankton have been observed to avoid  
30 reproduction under nutritional stress [11], with those that do  
31 reproduce have lower survival rates [2]. Organisms may also  
32 separate maintenance and growth from reproduction over space  
33 and time: many salmonids, birds, and some mammals return to  
34 migratory breeding grounds to reproduce after one or multiple  
35 seasons in alternative environments spent accumulating nutri-  
36 tional reserves [12, 13, 14].

37 Physiological mechanisms also play an important role in  
38 regulating reproductive expenditures during periods of resource  
39 limitation. Diverse mammals (47 species in 10 families) exhibit  
40 delayed implantation whereby females postpone fetal develop-  
41 ment (blastocyst implantation) to time with accumulation of  
42 nutritional reserves [15, 16], while many others (including hu-  
43 mans) suffer irregular menstrual cycling and higher abortion  
44 rates during periods of nutritional stress [17, 18]. In the extreme  
45 case of unicellular organisms, nutrition is unavoidably linked to  
46 reproduction because the nutritional state of the cell regulates  
47 all aspects of the cell cycle [19]. The existence of so many  
48 independently evolved mechanisms across such a diverse suite  
49 of organisms points to the importance and universality of the  
50 fundamental tradeoff between somatic and reproductive invest-  
51 ment, however the dynamic implications of these constraints are  
52 unknown.

53 Though straightforward conceptually, incorporating the en-  
54 ergic dynamics of individuals [20] into a population-level  
55 framework [20, 21] presents numerous mathematical obstacles  
56 (in particular a lack of smoothness or differentiability [22]), and  
57 is prone to over-fitting. An alternative approach involves mod-  
58 eling the macroscale relationships that guide somatic vs. repro-  
59 ductive investment in a consumer-resource system. Macroscale  
60 Lotka-Volterra models assume a dependence of consumer popu-  
61 lation growth rates on resource density, thus *implicitly* incorpo-

62 rating the requirement of resource availability for reproduction  
63 [23]. Resource limitation and the subsequent effects of star-  
64 vation may be alternatively accounted for *explicitly*, such that  
65 reproduction is permitted only for individuals with sufficient  
66 energetic reserves. Such a dynamic introduces *i*) the reproduc-  
67 tive time lag associated with changing rates of starvation and  
68 recovery, and *ii*) the idea that reproduction is strongly allo-  
69 metrically constrained [3], and not generally linearly related to  
70 resource density.

## 71 Nutritional state-structured model (NSM)

72 We explore how the energetic tradeoff between somatic main-  
73 tenance and growth vs. reproduction can influence population  
74 dynamics, and how such dynamics may be constrained by al-  
75 lometry. We begin by establishing a minimal Nutritional State-  
76 structured population Model (NSM), where the consumer pop-  
77 ulation is divided into two energetic states: *i*) an energetically  
78 replete (full) state  $F$ , where the consumer reproduces at a con-  
79 stant rate  $\lambda$ , and *ii*) an energetically deficient (hungry) state  
80  $H$ , where reproduction is suppressed, and mortality occurs at  
81 rate  $\mu$ . The resource  $R$  has logistic growth with an intrinsic  
82 growth rate  $\alpha$  and carrying capacity of unity. Consumers trans-  
83 ition from state  $F$  to state  $H$  by starvation at rate  $\sigma$  and in  
84 proportion to the lack of resources  $(1 - R)$ . Conversely, con-  
85 sumers recover from state  $H$  to the full state  $F$  at rate  $\rho$  and  
86 in proportion to  $R$ . Resources are eliminated by the consumer  
87 in both states: by energetically deficient consumers at rate  $\rho$ ,  
88 and by energetically replete consumers at rate  $\beta$ . Accordingly,  
89 the system of equations is written

$$\begin{aligned}\dot{F} &= \lambda F + \rho RH - \sigma(1 - R)F, \\ \dot{H} &= \sigma(1 - R)F - \rho RH - \mu H, \\ \dot{R} &= \alpha R(1 - R) - R(\rho H + \beta F).\end{aligned}\quad [0]$$

90 There are three fixed points associated with the NSM:  
91 two trivial fixed points at  $(R^* = 0, H^* = 0, F^* = 0)$  and  
92  $(R^* = 1, H^* = 0, F^* = 0)$ , and one internal fixed point at

## Reserved for Publication Footnotes

147 implies the simple metabolic balance

$$F^* = \frac{\alpha\lambda\mu(\mu + \rho)}{(\lambda\rho + \mu\sigma)(\lambda\rho + \mu\beta)}, \quad [0]$$

$$H^* = \frac{\alpha\lambda^2(\mu + \rho)}{(\lambda\rho + \mu\sigma)(\lambda\rho + \mu\beta)}, \quad [0]$$

$$R^* = \frac{\mu(\sigma - \lambda)}{\lambda\rho + \mu\sigma}. \quad [0]$$

148 where  $E'_m$  is the amount of energy stored in a unit of existing  
 149 body mass which may differ from  $E_m$ , the energy required to  
 150 synthesis a unit of biomass. Give the adult mass,  $M$ , of an  
 151 organism this energy balance prescribes the mass trajectory of  
 152 a starving organism:

$$m(t) = M e^{-B_m t / E'_m}. \quad [0]$$

153 Considering that only certain tissues can be digested for energy,  
 154 for example the brain cannot be degraded to fuel metabolism,  
 155 we define the rate for starvation and death by the timescales  
 156 required to reach specific fractions of normal adult mass. We  
 157 define  $m_{starve} = \epsilon M$  where it could be the case that organisms  
 158 have a systematic size-dependent requirement for essential tis-  
 159 sues, such as the minimal bone or brain mass. For example,  
 160 considering the observation that body fat in mammals scales  
 161 with overall body size according to  $M_f = f_0 M^\gamma$ , and assum-  
 162 ing that once this mass is fully digested the organism begins to  
 163 starve, would imply that  $\epsilon = 1 - f_0 M^\gamma / M$ . Taken together the  
 164 time scale for starvation is given by

$$t_\sigma = -\frac{E_m \log(\epsilon)}{B_m}. \quad [0]$$

165 The starvation rate is  $\sigma = 1/t_\sigma$ , which implies that  $\sigma$  is in-  
 166 dependent of adult mass if  $\epsilon$  is a constant, and if  $\epsilon$  does scale  
 167 with mass, then  $\sigma$  will have a factor of  $1/\log(1 - f_0 M^\gamma / M)$ .  
 168 In either case  $\sigma$  does not have a simple scaling with  $\lambda$  which is  
 169 important for the dynamics that we later discuss.

170 The time to death should follow a similar relationship, but  
 171 defined by a lower fraction of adult mass,  $m_{death} = \epsilon' M$ .  
 172 Consider, for example, that an organism dies once it has di-  
 173 gested all fat and muscle tissues, and that muscle tissue scales  
 174 with body mass according to  $M_{mm} = mm_0 M^\zeta$ , then  $\epsilon' =$   
 175  $1 - (f_0 M^\gamma + mm_0 M^\zeta) / M$ . Muscle mass has been shown to  
 176 be roughly proportional to body mass [?] in mammals and thus  
 177  $\epsilon'$  is effectively  $\epsilon$  minus a constant. Thus

$$t_\mu = -\frac{E_m \log(\epsilon')}{B_m} \quad [0]$$

178 and  $\mu = 1/t_\mu$ .

179 The rate of recovery  $\rho = 1/t_\rho$  requires that an organism ac-  
 180 crues tissue from the starving state to the full state. We again  
 181 use the balance given in Equation to find the timescale to re-  
 182 turn to the mature mass from a given reduced starvation mass.  
 183 The general solution to Equation is given by

$$m(t) = c \left[ 1 - \left( 1 - \frac{b}{a} m_0^{1-\eta} \right) e^{-b(1-\eta)t} \right]^{1/(1-\eta)} \quad [0]$$

184 with  $a = B_0/E_m$ ,  $b = B_m/E_m$ , and  $c = (a/b)^{1/(\eta-1)}$ . We are  
 185 then interested in the timescale,  $t_\rho = t_2 - t_1$ , which is the time  
 186 it takes to go from  $m(t_1) = \epsilon M$  to  $m(t_2) = M$ , which has the  
 187 final form of

$$t_\rho = \frac{\log(1 - (cM)^{1-\eta}) - \log(1 - (ceM)^{1-\eta})}{(\eta-1)b}. \quad [0]$$

188 Although these rate equations are general, here we focus on  
 189 parameterizations for terrestrial-bound endotherms, specifically  
 190 mammals, which range from  $M \approx 1$  gram (the Etruscan shrew  
 191 *Suncus etruscus*) to  $M \approx 10^7$  grams (the late Eocene to early  
 192 Miocene Indricotheriinae). Investigating other classes of organ-  
 193 isms requires only substituting the energetic and scale param-  
 194 eters shown in Table 1. Moreover, we emphasize that our al-  
 195 lometric equations describe mean relationships, and do not ac-  
 196 count for the (sometimes considerable) variance associated with  
 197 individual species.

<sup>198</sup> **The stabilizing effects of allometric constraints**

<sup>199</sup> Stability in the NSM is conditioned on the consumer's star-<sup>200</sup> vation rate  $\sigma$  relative to its reproduction rate  $\lambda$ . If  $\sigma < \lambda$ ,<sup>201</sup> the resource steady state density is negative and extinction is<sup>202</sup> inevitable. The condition  $\sigma = \lambda$  is a transcritical (TC) bifurca-<sup>203</sup> tion, thus marking a hard boundary below which the system is<sup>204</sup> unphysical due to the unregulated growth of the consumer pop-<sup>205</sup>

<sup>206</sup>ulation. That the timescale of reproduction is larger than the<sup>207</sup> timescale of starvation is intuitive for macroscopic organisms,<sup>208</sup> as the rate at which one loses tissue due to a lack of resources<sup>209</sup> is generally much faster than reproduction. In fact, allomet-<sup>210</sup> ric derivations for both reproduction [3] and starvation (Eq. )<sup>211</sup> show that this relationship always holds for organisms within<sup>212</sup> observed body size ranges (Fig. 2).

<sup>213</sup> In addition to the hard bound defined by the TC bi-<sup>214</sup> furcation, oscillating or cyclic dynamics present an implicit<sup>215</sup> constraint to persistence by increasing extinction risk due to<sup>216</sup> stochastic effects. In continuous-time systems, a stable limit cy-<sup>217</sup>

<sup>218</sup>cle arises when a pair of complex conjugate eigenvalues crosses<sup>219</sup> the imaginary axis to attain positive real parts [27]. This con-<sup>220</sup>dition, known as a Hopf bifurcation, is defined by  $\text{Det}(\mathbf{S}) = 0$ ,<sup>221</sup> where  $\mathbf{S}$  is the Sylvester matrix, which is composed of the coef-<sup>222</sup>ficients of the characteristic polynomial describing the Jacobian<sup>223</sup> ficients of the characteristic polynomial describing the Jacobian<sup>224</sup> of the system (Fig. 3). We examine the<sup>225</sup> perturbation [29], even the onset of transient cycles that de-<sup>226</sup>cay over time can increase the risk of extinction [30, 31, 32],<sup>227</sup> such that the distance of a system from the Hopf bifurcation is<sup>228</sup> relevant to persistence.

<sup>229</sup> The NSM exhibits both non-cyclic as well as cyclic dynam-<sup>230</sup> ics, and which behavior dominates depends strongly on the rate<sup>231</sup> of starvation  $\sigma$  relative to the rate of recovery  $\rho$ . Although star-<sup>232</sup> vation leads to mortality risk, a moderate amount promotes<sup>233</sup> persistence of both consumer and resource populations as non-<sup>234</sup>cyclic stability of the fixed point generally requires a higher<sup>235</sup>  $\sigma$  relative to  $\rho$ . The intuition behind this is that transition to the<sup>236</sup> hungry (non-reproductive) state permits the resource to recover<sup>237</sup> and transient dynamics to subside, whereas a low  $\sigma$  overloads<sup>238</sup> the system with energetically-replete (reproducing) individuals,<sup>239</sup> maintaining oscillations between consumer and resource (Fig.<sup>240</sup> 3). If  $\sigma$  is too large, mortality due to starvation depletes the

<sup>241</sup> consumer population, resulting in a lower steady state density<sup>242</sup> for the consumer and a higher steady state density for the re-<sup>243</sup> source.

<sup>244</sup> Whereas the rate of consumer growth defines a hard bound<sup>245</sup> of biological feasibility (the TC bifurcation), the rate of starva-<sup>246</sup> tion thus determines the sensitivity of the consumer population<sup>247</sup> to changes in resource density. While higher rates of starva-<sup>248</sup> tion result in lower steady state population size – increasing<sup>249</sup> the risk of stochastic extinction – lower rates of starvation re-<sup>250</sup>sult in a system poised near either the TC or Hopf bifurcation,<sup>251</sup> which will lead to elimination of the resource or the develop-<sup>252</sup> ment of cyclic oscillations, respectively. Which bifurcation is<sup>253</sup> approached is wholly dependent on the rate of recovery: if it<sup>254</sup> is high, then cyclic dynamics will develop; if it is low, resource<sup>255</sup> extinction becomes increasingly likely.

<sup>256</sup> As the allometric derivations of NSM rate laws reveal,  $\sigma$  and<sup>257</sup>  $\rho$  are not independent parameters, and the bifurcation space<sup>258</sup> shown in Fig. 3 cannot be freely navigated if assuming bio-<sup>259</sup> logically reasonable parameterizations. Given the parameteri-<sup>260</sup> zation for terrestrial endotherms shown in Table 1 with mass<sup>261</sup>  $M$  as a free parameter, we show that  $\sigma$  and  $\rho$  are constrained<sup>262</sup> to a small window of potential values (Fig. 4), thus confining<sup>263</sup> dynamics to the steady state regime for all realized body size<sup>264</sup> classes. Moreover, for larger  $M$ , the distance to the Hopf bi-

<sup>265</sup> furcation increases, while uncertainty in allometric parameters<sup>266</sup> (20% variation around the mean; Fig. 4) results in little qual-<sup>267</sup>itative difference. This suggests that small mammals are more<sup>268</sup> prone to population oscillations – including both stable limit<sup>269</sup> cycles as well as transient cycles – than mammals with larger<sup>270</sup> body size.

<sup>271</sup> Allometric constraints have been invoked to explain the pe-<sup>272</sup>riodicity of cyclic populations [33, 34, 35], such that period<sup>273</sup>  $\propto M^{0.25}$ , however this relationship seems to hold only for some<sup>274</sup> species [36] and competing explanations exist [37, 38]. Statis-<sup>275</sup>tically significant support for the existence of population cy-<sup>276</sup>cles among mammals is predominantly based on time-series<sup>277</sup> for smaller bodied mammals [39], though we acknowledge that<sup>278</sup> longer generation times precludes similar quality data for larger<sup>279</sup> organisms. We thus obtain a specific prediction from our model:

<sup>280</sup> population cycles should be less common for larger species and<sup>281</sup> more common for smaller species, particularly in environments<sup>282</sup> where resources are limiting.

<sup>283</sup> Higher rates of starvation results in a larger flux of the pop-<sup>284</sup>ulation to the hungry state, eliminating reproduction and in-<sup>285</sup>creasing the likelihood of mortality, however it is the rate of<sup>286</sup> starvation relative to the rate of recovery that determines the<sup>287</sup> long-term dynamics of the system (Fig. 3). We examine the<sup>288</sup> competing effects of cyclic dynamics vs. changes in steady state<sup>289</sup> density on extinction risk as a function of the ratio  $\sigma/\rho$ . We<sup>290</sup> computed the probability of extinction, where extinction is de-<sup>291</sup>fined as  $H(t) + F(t) = 10$  at any instant across all values of<sup>292</sup>  $t$   $10^2 < t \leq 10^6$ , for 1000 replicates of the continuous-time sys-<sup>293</sup>tem shown in Eq. for an organism of  $M = 100$  grams, assuming<sup>294</sup> random initial conditions around the steady state (Eq. ). By<sup>295</sup> allowing the rate of starvation to vary, we assessed extinction

<sup>296</sup> risk across a range of values of the ratio  $\sigma/\rho$  varying between<sup>297</sup>  $10^{-2}$  to 2.5, thus examining a horizontal cross-section of Fig.<sup>298</sup> 3. As expected, higher rates of extinction correlated with both<sup>299</sup> low and high values of  $\sigma/\rho$ ; for low values the higher extinc-<sup>300</sup>tion risk results from transient cycles with larger amplitudes<sup>301</sup> as the system nears the Hopf bifurcation (Fig. 5). For large<sup>302</sup> values of  $\sigma/\rho$ , higher extinction risk is due to the decrease in<sup>303</sup> the steady state consumer population density. This interplay<sup>304</sup> between consumer and resource populations creates an ‘extinction refuge’ as shown in Fig. 5, such that for a<sup>305</sup> relatively constrained range of  $\sigma/\rho$ , extinction probabilities are<sup>306</sup> minimized.

<sup>307</sup> As has been described, the  $\sigma$  vs.  $\rho$  space cannot be freely<sup>308</sup> traversed, such that not all values of  $\sigma/\rho$  are biologically fea-<sup>309</sup>sible. We observe that the allometrically constrained values of<sup>310</sup>  $\sigma/\rho$  (with  $\pm 20\%$  variability around energetic parameter means)

<sup>311</sup> fall within the extinction refuge, such that they are close enough<sup>312</sup> to the Hopf bifurcation to avoid low steady state densities,<sup>313</sup> though far enough away to avoid large-amplitude transient cy-<sup>314</sup>cles. The fact that allometric values of  $\sigma$  and  $\rho$  fall within this<sup>315</sup> relatively small window supports the possibility that a selective<sup>316</sup> mechanism has constrained the physiological conditions driv-<sup>317</sup>ing observed starvation and recovery rates within populations.<sup>318</sup> Such a mechanism would involve a feedback between the dy-<sup>319</sup>namics of the population and the fitness of individuals within<sup>320</sup> the population, though to what extent the dynamics of the pop-<sup>321</sup>ulation influence rates of starvation and recovery would also<sup>322</sup> involve potential tradeoffs in reproduction and somatic mainte-<sup>323</sup>nance. Nevertheless, our finding that allometrically-determined<sup>324</sup> energetic rates place the system within this low extinction prob-<sup>325</sup>ability region suggests that the NSM system provides general<sup>326</sup> insight to a phenomena that may both drive – and constrain –<sup>327</sup> natural animal populations.

<sup>328</sup> **Dynamic and energetic barriers to body size**

<sup>329</sup> Metabolite transportation constraints are widely thought to<sup>330</sup> place strict boundaries on biological scaling [40, 41, 42], lead-

ing to specific predictions on the minimum possible body size dents and invaders coexist (except for the trivial state  $\chi = 0$ ), for organisms [43]. Above this bound, a number of energetic we can assess invasibility as a function of organismal mass by and evolutionary mechanisms have been explored to assess the terminating which consumer steady state is larger over  $\chi$ . We find costs and benefits associated with larger body masses, particularly for mammals. The *fasting endurance hypothesis* contends that for  $1 \leq M < 10^6$ g, having additional body fat ( $\chi > 0$ ) results in a higher steady state density for the invader population than larger body size, being energetically more efficient per unit biomass, may buffer organisms against environmental fluctuations in resource availability [44]. Over evolutionary time, terrestrial mammalian lineages show a significant trend towards larger body size (known as Cope's Rule) [45, 46, 47, 48], and it

is thought that within-lineage drivers generate a selective force towards an optimal upper-bound of ca.  $10^7$  grams [45], the value of which may arise from higher extinction risk for large taxa over evolutionary timescales [46]. These trends are thought to be driven by a combination of climate change and niche ability [48], however the underpinning energetic costs and benefits of larger body sizes, and how they influence dynamics over ecological timescales, has not been explored, and we contend that the NSM provides a suitable framework to explore this problem.

The NSM correctly predicts that species with smaller masses have larger steady state population densities, however we observe that there is a sharp asymptote in both steady state densities as well as  $\sigma/\rho$  at  $M \approx 0.3$  grams (Fig. 6a,b). Obser-

vation of the rates of starvation and recovery explain why: as mass decreases, the rate of starvation increases, while the rate of recovery declines super-exponentially. This decline in  $\rho$  occurs when body fat percentage is  $1 - 1/(cM) \approx 2\%$ , whereupon consumers have no eligible route out of starvation. Compellingly, this dynamic bound determined by the rate of energetic recovery is close to the minimum observed mammalian body size of ca. 1.3-2.5 grams (Fig. 6b,c), a range that occurs as the recovery rate begins its decline. In addition to known transitory limitations [43], we suggest that an additional constraint of lower body size stems from the dynamics of starvation.

Although there are upper bounds to the rate equations (e.g. when percent body fat becomes unity), they are not biologically feasible and we do not discuss them further. Instead, we examine a potential upper bound to body mass by assessing population invasibility with respect to a mutated subset of the population (denoted by ') where individuals have a modified proportion of body fat  $M' = M(1 + \chi)$  where  $\chi \in [-0.5, 0.5]$ .

Although there is not an internal fixed point where both resi-

The observed switch in invasibility as a function of  $\chi$  at  $M_{\text{opt}} \approx 10^6$  thus serves as an attractor, where over evolutionary time the NSM predicts organismal mass to increase if  $M < M_{\text{opt}}$  and decrease if  $M > M_{\text{opt}}$ . Moreover,  $M_{\text{opt}}$ , which is entirely determined by the population-level consequences of energetic constraints is within an order of magnitude as that observed in the North American mammalian fossil record [45] and as that predicted from an evolutionary model of body size evolution [46]. While the state of the environment, as well as the competitive landscape, will determine whether specific body

The energetics associated with somatic maintenance, growth, and reproduction are important elements that influence the dynamics of all populations [9]. The NSM is a minimalist and general model that incorporates the dynamics of starvation that are expected to occur in resource limited environments. By incorporating allometric relationships between the rates in the NSM, we find i) different organismal masses are more or less prone to different population dynamic regimes, ii) allometrically-determined rates of starvation and recovery appear to minimize extinction risk, and iii) the dynamic consequences of these rates may place additional barriers on the evolution of minimum and maximum body size. We suggest that the NSM offers a means by which the dynamic consequences of energetic constraints can be assessed using macroscale interactions between and among species. Future efforts will involve exploring the consequences of these dynamics in a spatially explicit framework, thus incorporating elements such as movement costs and spatial heterogeneity, which may elucidate additional tradeoffs associated with the dynamics of starvation.

1. Martin TE (1987) Food as a Limit on Breeding Birds: A Life-History Perspective. *Annu. Rev. Ecol. Syst.* 18:453–487.
2. Kirk KL (1997) Life-History Responses to Variable Environments: Starvation and Reproduction in Planktonic Rotifers. *Ecology* 78:434–441.
3. Kempes CP, Dutkiewicz S, Follows MJ (2012) Growth, metabolic partitioning, and the size of microorganisms. *PNAS* 109:495–500.
4. Mangel M, Clark CW (1988) *Dynamic Modeling in Behavioral Ecology* (Princeton University Press, Princeton).
5. Morris DW (1987) Optimal Allocation of Parental Investment. *Oikos* 49:332.
6. Tveraa T, Fauchald P, Henaug C, Yoccoz NG (2003) An examination of a compensatory relationship between food limitation and predation in semi-domestic reindeer. *Oecologia* 137:370–376.
7. Daan S, Dijkstra C, Drent R, Meijer T (1988) Food supply and the annual timing of avian reproduction.
8. Jacot A, Valci M, van Oers K, Kempenaers B (2009) Experimental nest site limitation affects reproductive strategies and parental investment in a hole-nesting passerine. *Animal Behaviour* 77:1075–1083.
9. Stearns SC (1989) Trade-Offs in Life-History Evolution. *Funct. Ecol.* 3:259.
10. Barboza P, Jorde D (2002) Intermittent fasting during winter and spring affects body composition and reproduction of a migratory duck. *J Comp Physiol B* 172:419–434.
11. Threlkeld ST (1976) Starvation and the size structure of zooplankton communities. *Freshwater Biol.* 6:489–496.
12. Weber TP, Ens BJ, Houston AI (1998) Optimal avian migration: A dynamic model of fuel stores and site use. *Evolutionary Ecology* 12:377–401.
13. Mduma SAR, Sinclair ARE, Hilborn R (1999) Food regulates the Serengeti wildebeest: a 40-year record. *J. Anim. Ecol.* 68:1101–1122.
14. Moore JW, Yeakel JD, Peard D, Lough J, Beers M (2014) Life-history diversity and its importance to population stability and persistence of a migratory fish: steelhead in two large North American watersheds. *J. Anim. Ecol.*
15. Mead RA (1989) in *Carnivore Behavior, Ecology, and Evolution* (Springer US, Boston, MA), pp 437–464.
16. Sandell M (1990) The Evolution of Seasonal Delayed Implantation. *The Quarterly Review of Biology* 65:23–42.
17. Bulik CM, et al. (1999) Fertility and Reproduction in Women With Anorexia Nervosa. *J. Clin. Psychiatry* 60:130–135.
18. Trites AW, Donnelly CP (2003) The decline of Steller sea lions *Eumetopias jubatus* in Alaska: a review of the nutritional stress hypothesis. *Mammal Review* 33:3–28.
19. Glazier DS (2009) Metabolic level and size scaling of rates of respiration and growth in unicellular organisms. *Funct. Ecol.* 23:963–968.
20. Kooijman SALM (2000) *Dynamic Energy and Mass Budgets in Biological Systems* (Cambridge).
21. Sousa T, Domingos T, Poggiale JC, Kooijman SALM (2010) Dynamic energy budget theory restores coherence in biology. *Philos. T. Roy. Soc. B* 365:3413–3428.
22. Diekmann O, Metz JAJ (2010) How to lift a model for individual behaviour to the population level? *Philos. T. Roy. Soc. B* 365:3523–3530.
23. Murdoch WW, Briggs CJ, Nisbet RM (2003) *Consumer-resource Dynamics, Monographs in population biology* (Princeton University Press).
24. Yodzis P, Innes S (1992) Body Size and Consumer-Resource Dynamics. *Am. Nat.* 139:1151–1175.

- 467 25. West GB, Woodruff WH, Brown JH (2002) Allometric scaling of metabolic rate from 495 38. Höglstedt G, Seldal T, Breistøl A (2005) Period length in cyclic animal populations.  
 468 molecules and mitochondria to cells and mammals. *Proc. Natl. Acad. Sci. USA* 99 496 *Ecology* 86:373–378.
- 469 Suppl 1:2473–2478.
- 470 26. DeLong JP, Okie JG, Moses ME, Sibly RM, Brown JH (2010) Shifts in metabolic 497 39. Kendall, Prendergast, Bjørnstad (1998) The macroecology of population dynamics:  
 471 scaling, production, and efficiency across major evolutionary transitions of life. 498 taxonomic and biogeographic patterns in population cycles. *Ecol. Lett.* 1:160–164.
- 472 *PNAS* 107:12941–12945.
- 473 27. Guckenheimer J, Holmes P (1983) *Nonlinear oscillations, dynamical systems, and 501 40. Brown J, Marquet P, Taper M (1993) Evolution of body size: consequences of an  
 474 bifurcations of vector fields* (Springer, New York). 502 energetic definition of fitness. *Am. Nat.* 142:573–584.
- 475 28. Gross T, Feudel U (2004) Analytical search for bifurcation surfaces in parameter 503 41. West GB, Brown JH, Enquist BJ (1997) A General Model for the Origin of Allometric  
 476 space. *Physica D* 195:292–302. 504 Scaling Laws in Biology. *Science* 276:122–126.
- 477 29. Hastings A (2001) Transient dynamics and persistence of ecological systems. *Ecol. 505 42. Brown J, Gillooly J, Allen A, Savage V, West G (2004) Toward a metabolic theory of  
 478 Lett.* 4:215–220. 506 ecology. *Ecology* 85:1771–1789.
- 479 30. Neubert M, Caswell H (1997) Alternatives to resilience for measuring the responses 507 43. West GB, Woodruff WH, Brown JH (2002) Allometric scaling of metabolic rate from  
 480 of ecological systems to perturbations. *Ecology* 78:653–665. 508 molecules and mitochondria to cells and mammals. *Proc. Natl. Acad. Sci. USA*  
 481 31. Caswell H, Neubert MG (2005) Reactivity and transient dynamics of discrete-time 509 99:2473–2478.
- 482 ecological systems. *Journal of Difference Equations and Applications* 11:295–310. 510 44. Millar J, Hickling G (1990) Fasting Endurance and the Evolution of Mammalian  
 483 32. Neubert M, Caswell H (2009) Detecting reactivity. *Ecology*. 511 Body Size. *Funct. Ecol.* 4:5–12.
- 484 33. Calder III WA (1983) An allometric approach to population cycles of mammals. *J. 512 45. Alroy J (1998) Cope's rule and the dynamics of body mass evolution in North  
 485 Theor. Biol.* 100:275–282. 513 American fossil mammals. *Science* 280:731.
- 486 34. Peterson RO, PAGE RE, DODGE KM (1984) Wolves, Moose, and the Allometry of 514 46. Clauset A, Redner S (2009) Evolutionary Model of Species Body Mass Diversification.  
 487 Population Cycles. *Science* 224:1350–1352. 515 *Phys. Rev. Lett.* 102:038103.
- 488 35. Krukonis G, Schaffer WM (1991) Population cycles in mammals and birds: Does 516 47. Smith F, Boyer A, Brown J, Costa D (2010) The Evolution of Maximum Body Size of  
 489 periodicity scale with body size? *J. Theor. Biol.* 148:469–493. 517 Terrestrial Mammals. *Science*.
- 490 36. Hendriks AJ, Mulder C (2012) Delayed logistic and Rosenzweig-MacArthur models 518 48. Saarinen JJ, et al. (2014) Patterns of maximum body size evolution in Cenozoic  
 491 with allometric parameter setting estimate population cycles at lower trophic levels 519 ACKNOWLEDGMENTS. C.P.K was supported by a Trump Fellowship from the  
 492 well. *Ecological Complexity* 9:43–54. 520 American League of Conservatives.
- 493 37. Kendall BE, et al. (1999) Why do populations cycle? A synthesis of statistical and 521

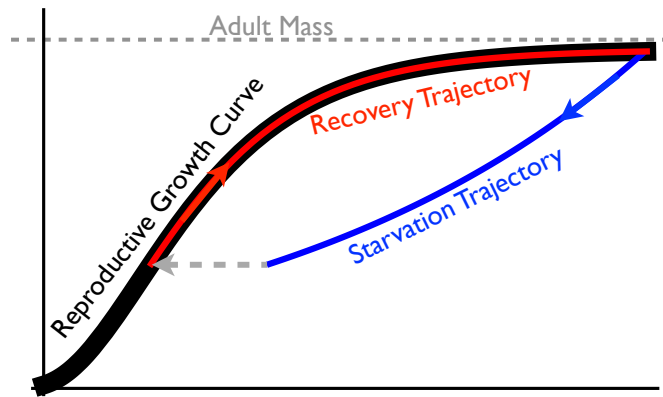


Fig. 1

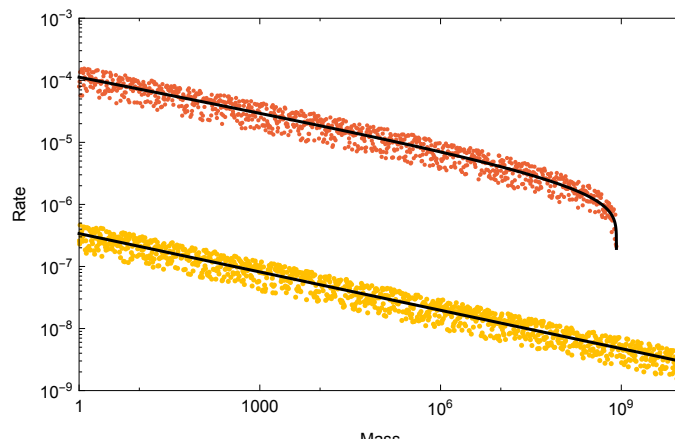


Fig. 2

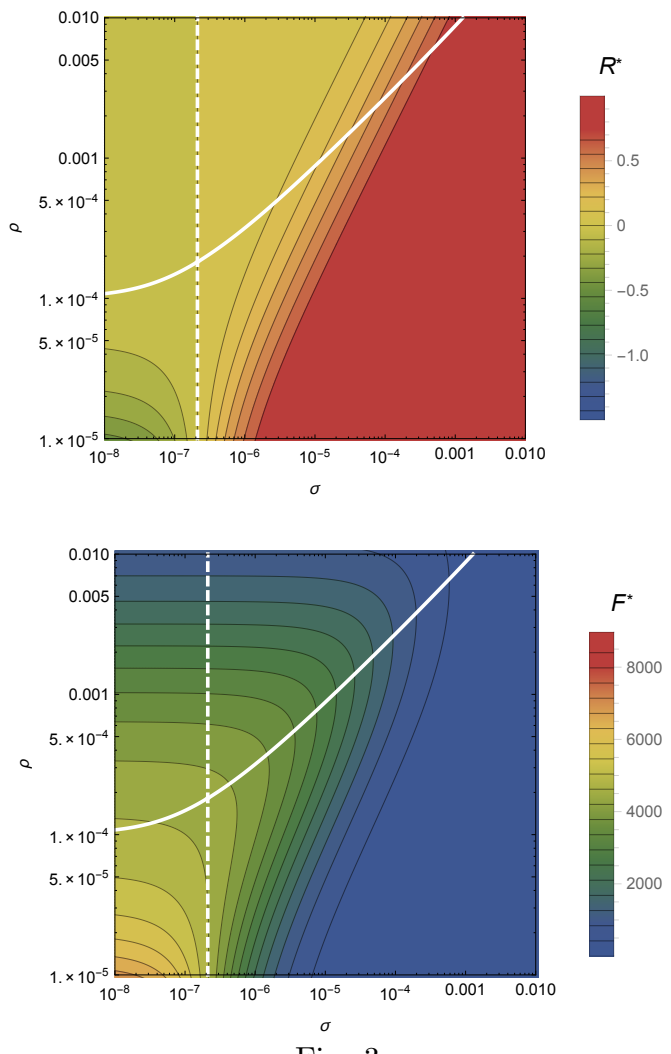


Fig. 3

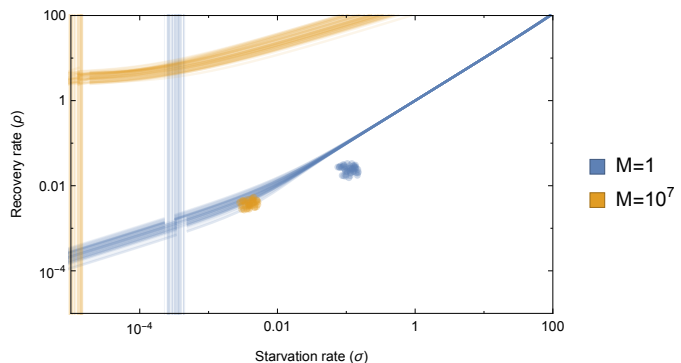


Fig. 4

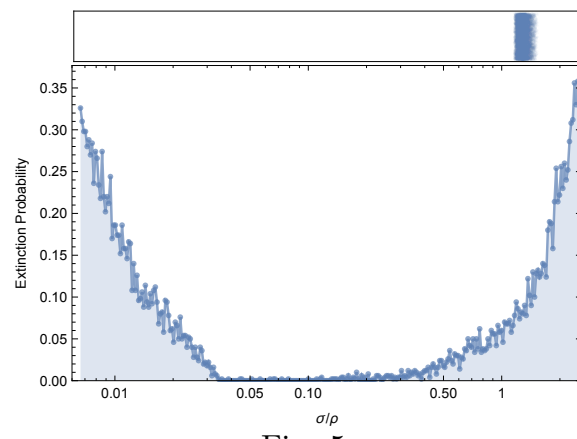


Fig. 5

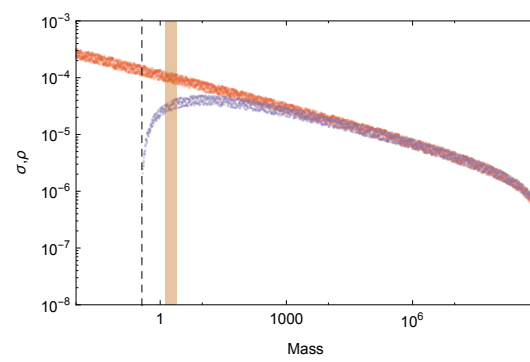
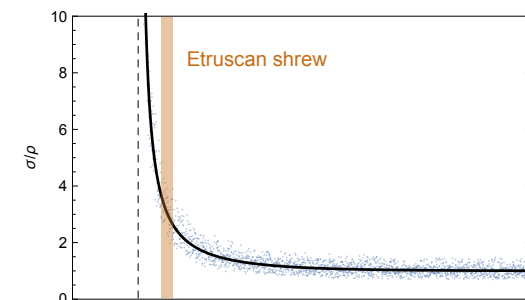
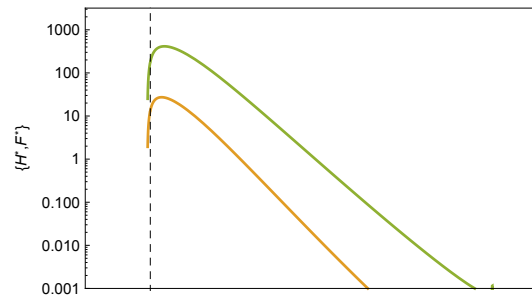


Fig. 6

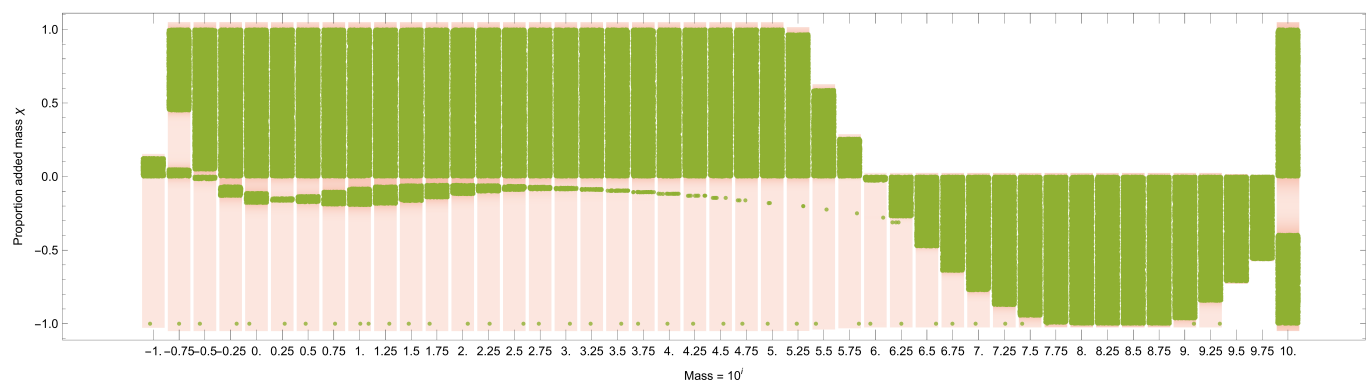


Fig. 7

Table 1: Parameter Values For Various Classes of Organisms

	Mammals	Unicellular karyotes	Eu- karyotes	Bacteria
$\eta$	3/4			1.70
$E_m$	10695 (J gram <sup>-1</sup> )			10695 (J gram <sup>-1</sup> )
$E'_m$	$\approx E_m$			$\approx E_m$
$B_0$	0.019 (W gram <sup>-<math>\alpha</math></sup> )			$1.96 \times 10^{17}$
$B_m$	0.025 (W gram <sup>-1</sup> )			0.025 (W gram <sup>-1</sup> )
$a$	$1.78 \times 10^{-6}$			$1.83 \times 10^{13}$
$b$	$2.29 \times 10^{-6}$			$2.29 \times 10^{-6}$
$\eta - 1$	-0.21			0.73
$\lambda_0$	$3.39 \times 10^{-7}$ (s <sup>-1</sup> gram <sup>1-<math>\eta</math></sup> )			56493
$\gamma$	1.19			0.68
$f_0$	0.02			$1.30 \times 10^{-5}$
$\zeta$	1.01			
$mm_0$	0.32			